Minimal ohmic contact resistance limits to *n*-type semiconductors

R. K. Kupka and W. A. Anderson
State University of New York at Buffalo, Department of Electrical and Computer Engineering, Center for Electronic and Electro-optic Materials, Bonner Hall, Amherst, New York 14260

(Received 12 October 1990; accepted for publication 12 December 1990)

An exact general formula for the lower contact resistance limit is derived, giving the lowest possible ohmic contact resistance for nondegenerate and degenerate metal-semiconductor contacts. Calculations for nondegenerate semiconductors include the nonparabolic nature of the conduction-band electrons and full Fermi–Dirac statistics. A discussion of standard emission theories shows that they are not applicable in the ohmic contact limit because of "electron tail lowering" and the negligence of quantum-mechanical reflections due to occupied states on the opposite side of their derivation. Together with a proof that an abrupt n-n^+ doping step is governed by thermionic emission, the ohmic contact resistance of a general ohmic contact is determined and it is shown that the n-n^+ doping step is responsible for this limitation. Thus, the lowest possible contact resistance is determined by the bulk doping of the semiconductor for a large variety of different alloyed and nonalloyed contact structures and not by the surface doping concentration. The theory predicts a lowest possible contact resistance in the 1×10^{-8} Ω cm^2 region for parabolic III-V semiconductors and of about 3×10^{-9} Ω cm^2 for Si and Ge.

I. INTRODUCTION

Ohmic contacts are of major importance for semiconductor devices. Considerable effort was spent in the past to find an optimal contact system for each semiconductor compound. Besides important properties like surface roughness, temperature stability, and aging behavior, the most important factor to evaluate ohmic contact systems is the specific contact resistance. The scaling down of Si very large scale integrated (VLSI) devices and the rapid development of III-V optical devices drew much emphasis on the development of low-resistance contacts. The present paper first provides a discussion of ohmic contact theories (Sec. II) and their limitations for low-resistance contacts (Sec. III). Then, an expression for a minimal possible contact resistance is derived (Sec. IV) together with the resistance of a high-low n-n^+ doping step (Sec. V), and the implication for the total ohmic contact resistance is discussed (Sec. VI) and compared with experimental data (Sec. VII). The importance of the high-low doping step is shown with proof that the minimal obtainable contact resistance is solely dependent on the semiconductor bulk doping and not on the surface doping concentration.

II. REVIEW OF THEORIES FOR OHMIC CONTACTS

Ohmic contacts usually employ degenerately doped semiconductor surface layers which were formed during the alloying process or were intentionally added by epitaxial growth or diffusion. The highly doped surface layer reduces the potential barrier thickness of the metal-semiconductor barrier which enables a strong tunneling current. Other conduction mechanisms like surface recombination or minority injection are by far less efficient than the tunneling currents and can be omitted. Dependent on the surface doping concentration, the metal-semiconductor contact exhibits either thermionic, thermionic field, or field emission. For thermionic field emission, the carriers tunnel at intermediate energies between the top of the potential barrier and the semiconductor Fermi level and field emission states that the carriers tunnel at the Fermi-level energy as shown in Fig. 1. Thus, field emission only occurs in degenerate semiconductors. Nondegenerate semiconductors have no allowed states at the Fermi-level energy; the next available states are at the conduction-band minimum above the Fermi level, and therefore nondegenerate semiconductors exhibit only field and thermionic field emission, but never field emission in the strong sense.

From early times, attempts were made to approximate the highly nonlinear transport properties in models. Analytical solutions of the emission integrals [the integral of all emission currents over energy: Eq. (1) in Sec. IV], assuming the WKB approximation for the tunneling of electrons, were derived by Stratton[1] for field emission into vacuum and by Padovani and Stratton,[2] and Stratton,[3,4] for thermionic field and field emission in metal-semiconductor barriers. The analytical expressions were obtained by expanding the tunneling barrier transmission probability at the emission maximum in a second-order Taylor series. The emission integral was then solved for field emission using only the first-order approximation of the tunneling probability and using the full second-order Taylor expansion for the thermionic field emission, resulting in fairly compact equations which enjoy frequent use up to the present. Yu[5] used the expressions in Refs. 1–4 to analytically calculate the ohmic contact resistance in metal-semiconductor barriers.

Because of the nonlinearity of the transport process, several numerical models have been used to describe the transport in the metal-semiconductor barrier. Crowell and Sze[6] numerically calculated the emission integral, assuming Boltzmann statistics and the necessary tunneling probabilities, including quantum-mechanical reflections of elec-

 0021-8979/91/063623-10$03.00

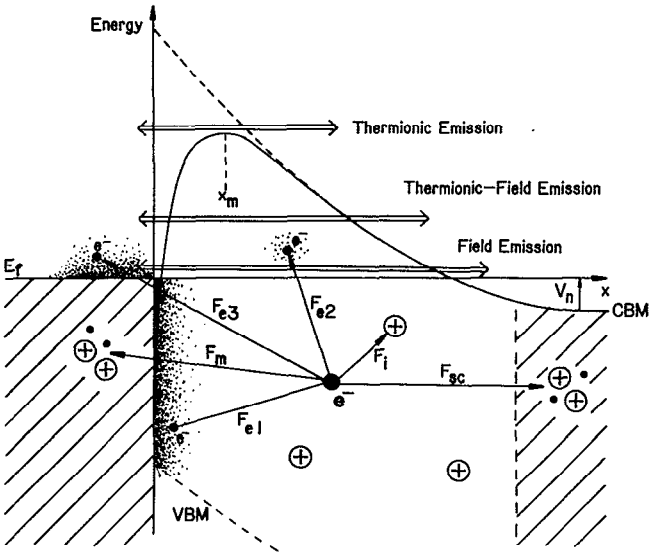

FIG. 1. Forces acting on an electron which partakes in the conduction process due to F_i: Impurities in the space-charge region; F_m: metal charge dipoles; F_{sc}: semiconductor charge dipoles; F_e: other free electrons.

trons which surmount the barrier, phonon optical backscattering of carriers, and also the influence of the diffusion process in the bulk semiconductor which supplies the junction with bulk carriers. All three are important for thermionic Schottky contacts especially in the low doping region, but become less important for tunneling contacts because of the strong tunneling currents and the smaller space-charge region. Chang and Sze[7] numerically integrated the emission integral using Fermi–Dirac statistics and an analytical WKB approximation for the tunneling probabilities. Chang, Fang, and Sze[8] used Ref. 7 to obtain specific contact resistances for Si and GaAs contacts, which shows that a limiting lowest contact resistance value exists. Also, the N_d^{-1} dependence of the contact resistance on the bulk doping concentration is implicitly shown.

Various progress in the theoretical understanding has been made since the development of these classical models.[1–8] A general Schottky contact is shown in Fig. 1. An electron in the space-charge region experiences a net sum of forces which determines the potential barrier shape. F_i is the interaction force between electron and fixed ionized impurities in the space-charge region and gives rise to the usual parabolic potential barrier. F_m is the interaction force between the emitted electron and all metal electron-nucleus dipoles which are constituted in such a way that a virtual mirror charge is generated. This gives rise to the image lowering potential. The electron also interacts with the electron-nucleus dipoles in the bulk semiconductor via the force F_{sc} which gives an additional mirror charge potential term. Since the distance from the emission plane x_m is very large, one can easily neglect this term without making any considerable error. The forces F_{e1}, F_{e2}, and F_{e3} are the interactions of the emitted electron with other emitted electrons, tunneling electrons within the space-charge region, and net excess tunneling electrons in the metal, respectively. Below the metal Fermi level, a large number of electrons tunnel into the semiconductor band gap with almost the same tunneling probability as conduction electrons and decay exponentially. Even though these electrons do not partake in the conduction process because no allowed states are present in the bulk semiconductor, they penetrate into the semiconductor and form a space-charge region, and the interaction force F_{e1} of the emitted electron with these electrons gives rise to an additional lowering term, the "electron tail lowering." The same is true for the interaction force F_{e2} with electrons above the metal Fermi level which partake in the conduction process. Since the density of these electrons decays exponentially with increasing energy, the potential contribution of F_{e2} is small and can be omitted. F_{e3} is the electron tunneling tail of semiconductor electrons from the conduction band into the metal which form an excess charge on the metal side of the contact. Because the tunneling electrons which give rise to the forces F_{e1}–F_{e3} carry a charge which lowers the potential barrier and, in turn, because of the different barrier shape, the tunneling behavior is affected and a self-consistent solution of Schrödinger's and Poisson's equations would be necessary as it is needed for quantum wells.

Pellegrini[9,10] analytically solved the metal-semiconductor emission integral, considering the F_i and all F_e forces by decoupling the Schrödinger–Poisson equation and deriving a potential lowering term which is then used in the current-voltage (I-V) and capacitance-voltage (C-V) equations with considerable success. Shenai and Dutton[11,12] employed a full numerical model including electron tail lowering, image lowering, using the WKB approximation, Fermi–Dirac statistics, and Franz's[13] expression for the kinetic energy of electrons. The theoretical predictions for thermionic and thermionic field emission in Shenai's paper are excellent and well matched to experimental results. The electron tail lowering is modeled by an exponential decaying potential term. Figure 2 shows the influence of the image and electron tail lowerings on the potential barrier of a GaAs Schottky contact with a doping concentration of $N_d = 10^{19}$ cm^{-3} using the potential terms from Shenai and Dutton in Ref. 11. It can be seen that the electron tail lowering considerably affects the barrier height considerably and that it is a much stronger effect than the image lowering. In Ref. 12 Shenai uses his model to calculate ohmic contact resistances and shows that the contact resistance values are usually much lower than predicted by the classical formulas in Ref. 5 because of the electron tail lowering.

Experimental measurements on alloyed GaAs contacts provided the evidence that the specific contact resistance is not dependent on the surface doping concentration, but rather on the bulk doping concentration of the semiconductor with ρ_c the specific contact resistance inverse proportional to the bulk doping concentration N_d. Braslau[14] showed the importance of the spreading resistance under the Ge-rich islands of a AuGeNi contact to GaAs and derived an expression which deviates from the usual N_d^{-1} dependence. Other models[15–20] ascribed the N_d^{-1} dependence to the doping high-low step under the contact.

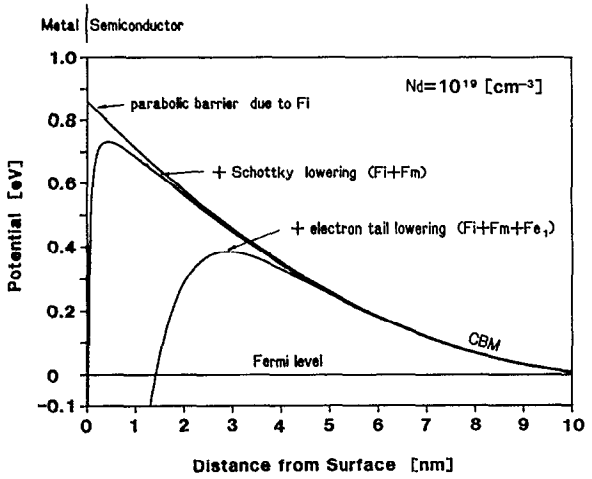

FIG. 2. Influence of the Schottky barrier lowering and the electron tail lowering on the potential barrier of a metal semiconductor contact with a doping concentration of $N_d = 1 \times 10^{19}$ cm^{-3}. The surface potential is taken to be 0.86 V, which relates to the Fermi-level pinning of a metal-GaAs contact. The potential terms are calculated from Refs. 11 and 12.

References 15–17 argued that thermionic emission over the doping high-low step is the prevailing conduction mechanism, whereas Refs. 18–20 assumed a diffusion-limited conduction process over the high-low step. In the present paper it is shown that the doping high-low step exhibits usual thermionic emission as assumed in Ref. 16, and a full degenerate calculation is carried out which extends the nondegenerate calculations in Refs. 15–17.

III. LIMITATION OF ANALYTICAL CONTACT RESISTANCE ESTIMATIONS

Frequently, Yu's[5] equations based on Refs. 1–4 are used to calculate the contact resistance of the metal-semiconductor interface which converge to zero contact resistance for low barrier heights. However, Refs. 1–4 have several inherent assumptions which limit the use of the models, especially for ohmic contacts.

(a) Quantum-mechanical reflections due to the occupancy probability in the opposite medium are neglected. For instance, an electron which is emitted at the Fermi-level energy would have a probability of $\frac{1}{2}$ of being scattered back in the opposite medium. This effect can be neglected for thermionic and thermionic field emission because the emission energy maximum is far above the Fermi level, but becomes increasingly important for degenerate semiconductors in the field-emission region and, thus, is very important for good ohmic contacts. Because of the small effective mass, III-V compounds become degenerate at moderate doping levels (3×10^{17} cm^{-3} for GaAs). Since the surfaces of good ohmic contacts are doped with much higher concentrations, the predicted currents in the classical model[5] are too high, and thus the calculated contact resistances for the metal-semiconductor barrier are lower than the actual values, if one considers the influence of this effect alone.

(b) The theories in Refs. 1–5 do not consider any barrier lowering effects. From the previous discussions, it is obvious that especially the electron tail lowering contributes a large barrier lowering potential as it can be seen in Fig. 2. For ohmic contacts, the barrier thickness is very small, which enables high tunneling conduction currents. Because the electrons which form the tails obey the same tunneling law as the electrons which partake in the conduction process, the electron tail lowering becomes more important as the contact is based on tunneling current transport. Thus, the classical formulas in Yu's paper[5] predict a much too high value of the contact resistance, and especially for very highly doped surface layers the use becomes ambiguous.

(c) Because the analytical expression of the electron tunneling probability in a Schottky barrier is singular for electrons which tunnel at the conduction-band minimum, no Taylor series expansion of the tunneling probability at the conduction-band minimum can be obtained and used in Refs. 1–4. Thus, the models in Refs. 1–5 do not give an explicit theory for nondegenerate semiconductors with emission maximum at the conduction-band minimum. This would be important for the description of nonalloyed nondegenerate ohmic contacts.

(d) The influence of the high-low doping step is not considered, and the theories in Refs. 1–5 only apply for the surface metal-semiconductor barrier. They do not describe the behavior of the complete ohmic contact system.

Because of the described inaccuracies of the analytical expressions, the equations in Ref. 5 are not used further to determine the exact contact resistance in a metal-semiconductor barrier, but we explore the lowest obtainable ohmic contact resistance limits, rather than absolute-resistance values.

IV. CALCULATION OF THE MINIMAL OHMIC CONTACT RESISTANCE IN METAL-SEMICONDUCTOR BARRIERS

A. Derivation

The semiconductor-metal current J_{sm} is given by

$$J_{sm}=q\int_{\mathbf{p}} v_x(\mathbf{p})T(\mathbf{p})[1-R(\mathbf{p})]n_p(\mathbf{p})d\mathbf{p}, \tag{1}$$

where n_p is the number of electrons per unit volume in phase space, v_x is the electron velocity in the x direction, $T(p)$ is the semiconductor-metal transmission probability, and $R(p)$ is the reflection probability in the metal. Using

$$n(\mathbf{p})=\frac{2}{h^3}f_s=\frac{2}{h^3}\frac{1}{1+e^{(|E|-E_f)/kT}}, \quad v_x=\frac{\partial E_x}{\partial p_x}, \tag{2}$$

one obtains

$$J_{sm}=2\frac{q}{h^3}\int_{E_x}\int_{p_y}\int_{p_z}\frac{T(|E|)[1-R(|E|)]dp_y\,dp_z}{1+e^{(|E|-E_f)/kT}}dE_x. \tag{3}$$

$|E|$ is the magnitude of the electron energy and f_s is the semiconductor Fermi–Dirac distribution. The reflection in the metal is given by the metal Fermi–Dirac distribution

$$R(|E|)=f_m=\frac{1}{1+e^{(|E|+qV-E_f)/kT}}, \tag{4}$$

which leads to the semiconductor-metal current J_{sm}:

$$J_{sm}=2\frac{q}{h^3}\int_{E_x}\int_{p_y}\int_{p_z}\frac{T(|E|)e^{(|E|+qV-E_f)/kT}dp_y\,dp_z}{(1+e^{(|E|-E_f)/kT})(1+e^{(|E|+qV-E_f)/kT})}\,dE_x. \tag{5}$$

Exchanging the direction of transport by switching the expressions for f_s and f_m gives the metal-semiconductor current J_{ms}. The total current J is

$$J=J_{sm}-J_{ms}=2\frac{q}{h^3}\int_{E_x}\int_{p_y}\int_{p_z}\frac{T(|E|)e^{(|E|-E_f)/kT}(e^{qv/kT}-1)dp_y\,dp_z}{(1+e^{(|E|-E_f)/kT})(1+e^{(|E|+qV-E_f)/kT})}\,dE_x. \tag{6}$$

Assuming parabolic and spherical bands with

$$E_{x,y,z}=\frac{p_{x,y,z}^2}{2m_e^*},\quad |E|=E_x+E_y+E_z, \tag{7}$$

and substituting

$$y^*=\frac{p_y}{(2m_e^*kT)^{1/2}},\quad z^*=\frac{p_z}{(2m_e^*kT)^{1/2}},\quad a=\frac{E_x-E_f}{kT},\quad \Psi=\frac{qV}{kT} \tag{8}$$

one obtains

$$J=\frac{4qm_e^*kT}{h^3}\int_{E_x}\int_{y^*=0}^{\infty}\int_{z^*=0}^{\infty}\frac{T(|E|)e^{a+y^{*2}+z^{*2}}(e^{\Psi}-1)dy^*\,dz^*}{(1+e^{a+y^{*2}+z^{*2}})(1+e^{a+y^{*2}+z^{*2}+\Psi})}\,dE_x. \tag{9}$$

Transferring into cylindrical coordinates gives

$$J=\frac{4\pi qm_e^*kT}{h^3}\times\int_{E_x}\int_{r=0}^{\infty}\frac{T(|E_x|)e^{a+r^2}(e^{\Psi}-1)2r\,dr}{(1+e^{a+r^2})(1+e^{1+r^2+\Psi})}\,dE_x. \tag{10}$$

The angular integration over 2π is already carried out, and the π is moved into the prefactor. The emission process takes place in the x direction, and thus only the x component of the energy determines the transmission probability $T(E)$. The prefactor can be rewritten with the usual expression for the effective Richardson constant A^*. Substituting $t=r^2$ gives

$$J=\frac{A^*T}{k}\int_{E_x}\int_{t=0}^{\infty}\frac{T(E_x)e^{a+t}(e^{\Psi}-1)dt}{(1+e^{a+t})(1+e^{a+t+\Psi})}\,dE_x, \tag{11}$$

and integration produces

$$J=\frac{A^*T}{k}\int_{E_x}T(E_x)\ln\left(\frac{1+e^{(E_x-E_f)/kT}}{e^{-qv/kT}+e^{(E_x-E_f)/kT}}\right)dE_x. \tag{12}$$

Only electrons with energies above the conduction-band minimum of the semiconductor can partake in the conduction process which gives the lower integration limit. Further, the transmission probability $T(E_x)$ can never be greater than 1, and setting T equal to 1 gives the highest obtainable current. Differentiation of Eq. (12) over V, exchanging the integration and differentiation order, and differentiating the integrand leads to

$$\rho_{c,\min}^{-1}=\left.\frac{dJ}{dV}\right|_{v\to 0}=\frac{qA^*}{k^2}\int_{E_x-E_f=qV_n}^{\infty}\frac{1}{1+e^{(E_x-E_f)/kT}}\,d(E_x-E_f). \tag{13}$$

The final minimal contact resistance $\rho_{c,\min}$ is

$$\rho_{c,\min}=\frac{k}{qA^*T}\frac{1}{\ln(1+e^{-qV_n/kT})}. \tag{14}$$

Even though the derivation was carried out for spherical semiconductors, it also holds for nonspherical semiconductors if one uses a different expression for A^* according to Refs. 21 and 22.

B. Approximation for nondegenerate semiconductors

For nondegenerate semiconductors with $V_n \gg kT/q$ and using the Boltzmann statistics, Eq. (14) can be approximated by

$$\rho_{c,\min}=\frac{k}{qA^*T}e^{qV_n/kT}=\frac{k}{qA^*T}\frac{N_c}{N_d}, \tag{15}$$

which verifies the known N_d^{-1} dependence of the contact resistance. N_c is the effective density of states in the conduction band, and N_d is the electrically active bulk doping concentration.

TABLE I. Nonparabolicity constants α and effective electron masses of different semiconductors.

Semiconductor	Si	Ge	GaAs	GaSb	InP	InAs	InSb	ZnS	ZnSe	ZnTe	CdTe
α (eV^{-1})	0.50	0.65	0.64	1.36	0.67	2.73	5.72	0.14	0.26	0.26	0.45
m^*_{CBM}/m_0	···	···	0.067	0.045	0.080	0.023	0.014	0.28	0.14	0.18	0.096

C. Approximation for degenerate semiconductors

For degenerate semiconductors, the nonparabolic nature of the conduction band must be considered. Taking the emission probability $f_s(1 - f_m)$ from (1) shows that the emission maximum is always at the Fermi energy level, if semiconductor states at the Fermi-level energy exist and we set the transmission probability equal to 1, as we have done above to obtain the minimal contact resistance. For degenerate semiconductors, this implies that the majority of the carriers are emitted with a different electron effective mass than the effective mass of the conduction-band minimum because the Fermi level lies deep in the conduction band and electrons at the Fermi level have an increased mass, according to their nonparabolicity. This changes the effective Richardson constant for these carriers. Nonparabolic calculations by Reggiani[23] give, for the effective mass of electrons which are at an energy of ΔE above the conduction-band minimum,

$$m_c^* = m^*_{CBM}(1 + 2\alpha\Delta E),$$
$$A^*_{np} = A_0 \frac{m_c^*}{m_0} = A^*(1 + 2\alpha\Delta E), \quad \Delta E > 0, \tag{16}$$

where m_c^* is the effective electron mass considering the nonparabolic conduction band, m^*_{CBM} is the conduction-band minimum effective mass of the semiconductor, α is a semiconductor compound specific constant, A_0 is the free-space Richardson constant, A^* is the usual effective Richardson constant of Eq. (11), A^*_{np} is for the nonparabolicity corrected effective Richardson constant, and m_0 is the free-space electron mass. The material-dependent constant α can be found for a semiconductor with a conduction-band minimum at the Γ point only with

$$\alpha_\Gamma = \frac{1}{E_\Gamma}\left(1 - \frac{m^*_\Gamma}{m_0}\right). \tag{17}$$

E_Γ is the direct energy gap, and m^*_Γ is the effective electron mass at the Γ point. Similar equations hold true for semiconductors with a conduction-band minimum at the L or X point and can be found in Reggiani[23] who also gives α values for various semiconductors which are listed in Table I. Using Eq. (16) in (14) gives, for degenerate semiconductors with $V_n < -kT/q$,

$$\rho_{c,\min} = \frac{k}{qTA^*[1 + 2\alpha(-qV_n)]}\left(\frac{kT}{-qV_n}\right). \tag{18}$$

D. Determination of Fermi-level potential V_n

To use Eqs. (18) and (14), the Fermi-level potential V_n for degenerate and nondegenerate semiconductors must be accurately determined. Using Fermi–Dirac statistics and allowing for nonparabolic conduction bands, the carrier concentration n in the semiconductor can be found by solving

$$n = N_c \frac{2}{\Gamma(1/2)} \int_{x=0}^{\infty} \frac{\sqrt{x}(1 + \beta x)^{3/2}}{1 + e^{x - \eta}}\, dx,$$
$$\eta = \frac{-qV_n}{kT}, \quad \beta = 2\alpha kT, \quad N_c = 2\left(\frac{2\pi kTm^*}{h^2}\right)^{3/2}, \tag{19}$$

where $\Gamma(x)$ is the gamma function. Expanding the bracket term in the integrand into a Taylor series in x, it can be shown that

$$n = N_c\left(F_{1/2}(\eta) + \frac{9\beta}{4}F_{3/2}(\eta) + \frac{45\beta^2}{32}F_{5/2}(\eta) - \frac{315\beta^3}{384}F_{7/2}(\eta)\ldots\right). \tag{20}$$

$F_j(\eta)$ is the Fermi–Dirac integral of order j:

$$F_j(\eta) = \frac{1}{j\Gamma(j)} \int_0^{\infty} \frac{x^j}{1 + e^{x - \eta}}\, dx. \tag{21}$$

For usual operating conditions, it is easy to show that only the first three terms in Eq. (20) contribute to the sum and defining a function $F_\alpha(\eta)$ with

$$F_\alpha(\eta) = F_{1/2} + \frac{9\beta}{4}F_{3/2}(\eta) + \frac{45\beta^2}{32}F_{5/2}(\eta) \tag{22}$$

makes it possible to determine the Fermi level potential V_n by solving the balance equation

$$N_c F_\alpha\left(-\frac{qV_n}{kT}\right) - \frac{N_{d0}}{1 + ge^{(\Delta E_d - qV_n)/kT}} = 0. \tag{23}$$

N_{d0} is the doping donor density of the semiconductor, ΔE_d is the impurity activation energy, and g is the degeneracy of the donor.

Solving Eq. (23) numerically to obtain the Fermi-level potential V_n and using the value in Eq. (14) gives the value for the lowest obtainable contact resistance of a metal-semiconductor barrier with N_{d0} semiconductor doping concentration. For degenerate semiconductors, A^* in Eq. (14) must be replaced with A^*_{np} of Eq. (16) as done for Eq. (18).

E. Results for common semiconductors

Assuming s-like donors with degeneracy factors of $g = 2$, activation energies ΔE_d according to the hydrogen atom model, nonparabolicity constants α, and effective electron masses according to Table I, and solving the Fermi–Dirac integral in Eq. (23) numerically, calculations have been carried out to estimate the lowest possible ohmic

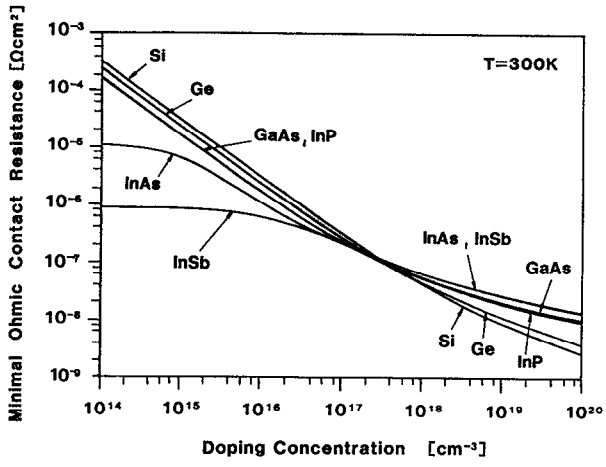

FIG. 3. Lower ohmic contact resistance limit for different semiconductors.

contact resistance with the use of Eq. (14). The results are depicted in Figs. 3 and 4. As discussed earlier, at nondegenerate doping concentrations, the contact resistance drops with N_d^{-1}, and the degenerate resistance limit deviates from this and tends to saturate. The InAs and InSb behavior at low doping concentration is due to the low electron-hole mass ratio and the small band gap which causes the Fermi-level potential to be always close to the conduction band. It must be pointed out that the obtained values are the lowest possible contact resistances and not the real contact resistances for metal-semiconductor contacts. For instance, a contact to Si with a doping concentration of $N_{d0} = 10^{15}$ cm^{-3} is, of course, a good Schottky diode and not an ohmic contact with resistance of 10^{-4} Ω cm^{-2}, the appropriate minimal value in Fig. 3. The tunneling probabilities $T(E)$ were set equal to 1 in the above derivation to obtain the limiting value of the contact resistance, an assumption which does not represent the actual physical picture. However, even by doping the surfaces extremely high and, thus, converging the tunneling

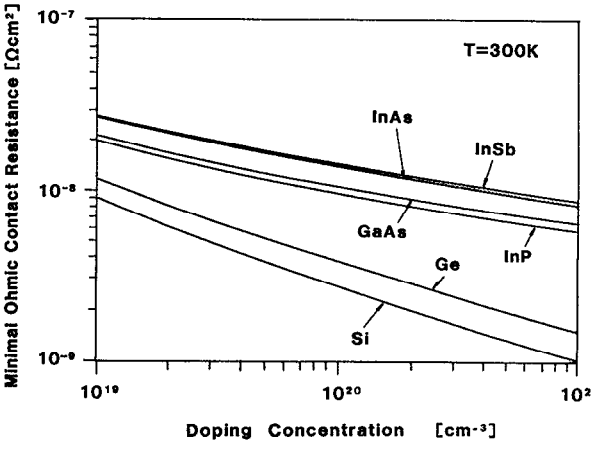

FIG. 4. Lower ohmic contact resistance limit for different semiconductors at very high doping concentrations.

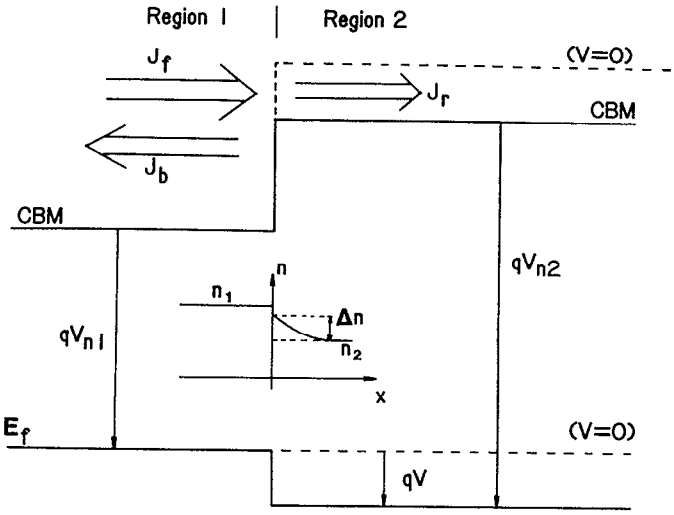

FIG. 5. Band diagram, currents, and excess carrier concentration for an $n - n^+$ junction (doping step). Position of the conduction-band minimum (CBM) and the Fermi level (E_f).

probabilities to 1 and forming an ohmic contact, Eq. (14) states that a specific, material, and doping-dependent contact resistance limit exists which cannot be surpassed. The above derivation is, in the strong sense, only valid for uniformly doped semiconductors and not for contacts with degenerately doped surface layers. It is shown in the following that a nonuniform doping concentration under the contact affects the ohmic contact resistance in such a way that the limit of Eq. (14) holds. This is because an $n - n^+$ doping step junction is formed which behaves in such a way that Eq. (14) is valid.

V. CARRIER TRANSPORT IN THE HIGH-LOW JUNCTION

Figure 5 depicts the energy-band diagram for a semiconductor $n^+ - n$ doping step assuming nondegenerate semiconductors and a doping step transition region of Δx. First, we consider an abrupt doping step with $\Delta x = 0$. As in a Schottky barrier, thermionic emission takes place. The forward current J_f injects carriers to the edge of the depletion region and causes an excess carrier buildup of $n_{02} + \Delta n$ there. These excess carriers are swept away from the depletion region edge by the recombination current J_r and because of the sign of the electric field in th field region is partly emitted back into the depletion region, forming one part of the backward current J_b. The other part of J_b is formed by the usual equilibrium emission rate of semiconductor 2. Writing down the expressions for the currents gives

$$J_f = A^* T^2 e^{-q(V_{n2} - V)/kT},$$
$$J_b = A^* T^2 e^{-qV_{n2}/kT} + q\Delta n v_b, \tag{24}$$
$$J_r = K_{\text{maj,min}} \Delta n.$$

Δn is the excess carrier density, v_b is the emission velocity, and $K_{\text{maj,min}}$ are constants which depend on the carrier conduction process in region 2 and are

$$K_{\text{min}}=\frac{qD_n}{L_n},\quad K_{\text{maj}}=\frac{qD_n}{L_d}=\frac{kT\mu_n}{L_d}. \tag{25}$$

L_d is the Debye length in region 2, L_n is the diffusion length, and D_n is the diffusion constant. If the electrons are majority carriers in region 2 as in the n-n_+ junction, then K_{maj} has to be used because the current transport is due to strong electric fields, whereas if the electrons are minority carriers in region 2, as it is for a p-n junction, then J_r is a pure diffusion current and K_{min} must be used in Eq. (24). Reference 6 gives, for v_b,

$$v_b=\frac{A^*T^2}{qN_c}. \tag{26}$$

Using Eqs. (26) and (25) in (24) gives, for the recombination current which is the real measurable current in the junction,

$$J_r=J_f-J_b=\frac{e^{-qV_{n2}/kT}(e^{qV/kT}-1)}{(1/A^*T^2)+(1/K_{\text{maj,min}}N_c)}. \tag{27}$$

If $A^*T^2 > K^*N_c$, then J_f is higher than the possible recombination current. This leads to a buildup of excess carriers at the edge of the depletion region which increases J_b due to the back emission of excess carriers until equilibrium is reached. Thus, for small J_r, the carriers are in equilibrium with medium 1 at the depletion region edge in medium 2, as is the case for the classical p-n junction, and Eq. (27) becomes the usual p-n expression. If $A^*T^2 < K^*N_c$, then the removal of carriers from the depletion region edge is faster than the supply by J_f and the junction is emission limited. This is usually the case for n-n^+ junctions, and Eq. (27) becomes the well-known thermionic expression. Calculating the conditions

$$A^*T^2 < K_{\text{maj}}N_c=qN_c\mu\sqrt{\frac{kTN_{d2}}{\epsilon_s}},$$

$$A^*T^2 < K_{\text{min}}N_c=\sqrt{\frac{qkT\mu}{\tau_n}}N_c, \tag{28}$$

with N_{d2} the doping concentration in region 2 and τ_n equal 1 ns (for GaAs), one can test whether a junction is diffusion limited. Using Eq. (28), it can be shown that the n-n^+ GaAs junction is limited by thermionic emission for carrier densities $N_{d2} > 10^{15}$ cm^{-3}. Therefore, thermionic emission is the prevalent transport mechanism in n-n^+ junctions because ohmic regions in semiconductors are much higher doped than this value. Even though the derivation was carried out for nondegenerate semiconductors, it also holds for degenerate semiconductors if the degenerate values for the diffusion constants and lengths in Eq. (25) are chosen.

Comparing Fig. 5 with Fig. 1 shows that virtually no difference exists between the n-n^+ junction and the previously discussed Schottky barrier. The high-low doping step is a Schottky junction without a potential barrier. The previously derived equation for the ohmic contact resistance limit of metal-semiconductor junctions is therefore directly usable for the n-n_+ step, and Figs. 3 and 4 automatically give the (exact) contact resistance of a high-low doping step assuming both work on thermionic emission. The semiconductor region with the highest Fermi potential V_n (V_{n2} in Fig. 5) is chosen for the necessary variable in Eq. (14). If, for some reason, the transport process is not thermionic, then Eq. (27) states that the currents would be smaller as for thermionic transport, and thus the ohmic contact resistance of the n-n^+ junction would increase.

So far, we have only considered an abrupt n-n^+ step. If the transition is gradual within a length of Δx, then an exact calculation of the transport properties becomes very difficult. One can, however, give a rough estimate at what n-n^+ transition length an influence on the electrical characteristic can be expected. The electric field in the transition region is about $E = (V_{n2} - V_{n1})/\Delta x$. The time needed for the carriers to pass through the transition region due to the built-in field is $t_{\text{pass}} = \mu E/\Delta x$. E is the electric field, and μ is the electron mobility. Thermionic emission holds if the electrons do not change the energy in the transition region due to inelastic scattering. With the energy relaxation time τ_E, one can assume that thermionic emission occurs for

$$\Delta x < \sqrt{\tau_E\mu(V_{n2}-V_{n1})}. \tag{29}$$

The energy relaxation time for GaAs is from Ref. 23 about 10^{-12} s and close to this value for other semiconductors. Since ionized impurity scattering is assumed to be elastic, the energy relaxation time is independent of the doping concentration. Calculating Eq. (29) for a realistic potential step difference of 26 meV gives a maximal transition region Δx of about 120 nm for GaAs and 40 nm for Si. Usual transition regions in doping steps of ohmic contact are well below this length, and thus thermionic emission is responsible for the current transport in ohmic contact high-low doping steps. If the doping step transition length Δx is above the value calculated in Eq. (29), then the above theory becomes inaccurate and further research would be necessary on the transport properties of the n-n^+ step.

VI. TOTAL CONTACT RESISTANCES OF OHMIC CONTACTS

A usual ohmic contact consists of a highly doped surface layer on a bulk semiconductor. The band diagram under bias is depicted in Fig. 6 where the thickness of the highly doped surface layer is t_{sp}, the thickness of the metal semiconductor potential barrier is t_{dr}, and the length of the n-n^+ doping step transition region is Δx. The current from the metal into region 2 is the sum of two current contributions J_{fm} and F_{fs}. For the first, the carriers from region 1 are not scattered passing the surface doping region and are in equilibrium with the metal Fermi level even though they are situated at the edge of region 2. The second current is due to the scattered carriers and obeys the Fermi level in the surface layer. Defining a constant c between 0 and 1, the total current is the sum

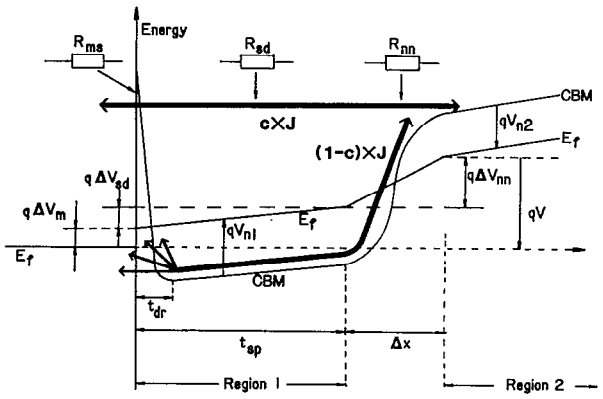

FIG. 6. Band diagram of an ohmic contact with a highly doped surface region. Dependent on the thickness t_{sp} of the surface region, the metal-semiconductor surface region contact resistance R_{ms}, the ohmic surface region resistance R_{sd}, and the doping step resistance R_{nn} become more or less influential. The minimal total resistance is given by R_{nn}. A voltage drop in the semiconductor bulk region behind the doping step is not considered.

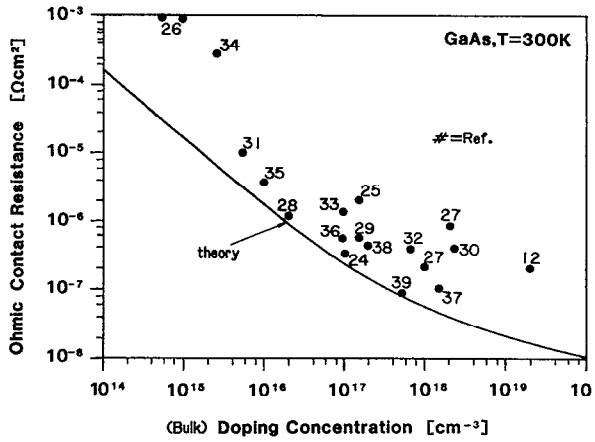

FIG. 7. Theoretical contact resistance limits for GaAs calculated from Eqs. (14) and (23) in comparison with experimental values of vastly different contact structures.

$$J_{tot}=cJ_{fm}+(1-c)J_{fs}. \tag{30}$$

For the scattered carriers, three contact resistances are connected in series and their influence varies with different t_{sp}. R_{ms} is the metal-semiconductor contact resistance, R_{sd} is the semiconductor surface doping resistance due to the usual ohmic resistance of bulk semiconductors, and R_{nn} is the n-n^+ doping step resistance. The total current is therefore

$$I_{tot}=\frac{cV}{R_{nn}}+(1-c)\left(\frac{\Delta V_m}{R_{ms}}+\frac{\Delta V_{sd}}{R_{sd}}+\frac{\Delta V_{nn}}{R_{nn}}\right), \tag{31}$$

which is equivalent to the circuit diagram in Fig. 6. As shown above, electrons which pass the metal-semiconductor or n-n^+ potential barrier are transported away by strong majority currents in the semiconductor regions and need several Debye lengths to reach equilibrium. This gives the following dependence of the total contact resistance R_{tot} on t_{sp}.

(a) $t_{dr} > t_{sp}$, $c=1$: The surface doping layer is too thin and part of the metal-semiconductor depletion region extends into the bulk semiconductor. The total contact resistance is determined by tunneling into region 2. Because of the increased thickness of the barrier, the resistance is much larger than the minimal value R_{nn} according to Eq. (29).

(b) $t_{dr}=t_{sp}$, $c=1$: The surface doping layer fits completely into the metal-semiconductor potential barrier, the contact resistance is given by $R_{tot}=R_{nn}$, and Eq. (14) can be used (with $V_n=V_{n2}$) for R_{nn}.

(c) t_{dr} very large, $c=0$: The carriers find equilibrium in the surface doping layer, all three contact resistances are in series, and $R_{tot}=R_{ms}+R_{sd}+R_{nn}$. Because of the high doping in region 1, the ohmic resistance R_{sd} can be neglected, and also, according to Eq. (14), $R_{ms} < R_{nn}$. The total resistance is therefore $R_{tot} > R_{nn}$.

(d) t_{dr} intermediate $0<c<1$: Here, the electrons do not find equilibrium in the surface doping layer, and some of the emitted electrons from the metal reach material 2 directly without significant scattering in the surface layer, whereas others are scattered and are in equilibrium with the surface layer Fermi level. Taking Eq. (31), $R_{tot} \geqslant R_{nn}$ for all possible c and resistances.

This proves that the minimal obtainable contact resistance is determined by the emission into region 2, the bulk semiconductor. Equations (23) and (14) give the lowest possible contact resistance for any type of ohmic contact if one uses the semiconductor bulk values for the calculation parameter. It also must be pointed out that the above derivation is also applicable if the degenerate layer is of a different semiconductor type, since no assumptions were made whether the regions are of the same semiconductor compound.

VII. EXPERIMENTAL DATA

Figure 7 shows the calculated minimal contact resistance, using Eqs. (14) and (29), for GaAs together with the experimental contact resistances of Table II. Only contact resistance values which come close to the resistance limit were included in Table II. The measured resistance values verify Eq. (14). This is remarkable since the involved contacts are not only standard (alloyed) contacts with degenerately doped surface, but are also nonalloyed,[12,37-39] heterojunctions,[37] graded $In_xGa_{1-x}As$ layers,[38] or strained layer superlattices.[39] To verify the present theory, further experiments would have to be carried out at bulk doping concentrations of above 10^{19} cm^{-3}. Two reported values in the literature do not fit with the current theory. The first[40] reports a contact resistance of 5×10^{-9} Ω cm^2 for an $In_xGa_{1-x}As$ graded gap contact with doping concentration of 1×10^{19} cm^{-3} and uses the circular method of Cox and Strack to measure this extremely low contact resistance. The second[41] employs an InAs cap layer on InGaAs and obtains a 1.7×10^{-8} Ω cm^2 resistance at a bulk doping of 1×10^{18} cm^{-3}.

TABLE II. Experimental values of different n-GaAs contact systems.

Contact system	Contact resistance ($\Omega\,cm^2$)	Bulk doping (cm^{-3})	Reference	Remark
AuGeNi	2×10^{-7}	2×10^{19}	12	nonalloyed
AuGeNi	2.9×10^{-7}	1×10^{17}	24	alloyed, surface ion implanted
InPt	2×10^{-6}	1.5×10^{17}	25	alloyed
AgInGe	1×10^{-3}	5×10^{14}	26	alloyed, early contact
AgInGe	9×10^{-4}	1×10^{15}	26	alloyed
InPd	8×10^{-7}	2×10^{18}	27	alloyed
PdGeIn	2×10^{-7}	1×10^{18}	27	alloyed
AuGeNi	1×10^{-6}	2×10^{16}	28	alloyed
AuGeNi	5×10^{-7}	1.5×10^{17}	29	alloyed
AuGeNi	4×10^{-7}	2.2×10^{18}	30	alloyed, RTA
AuGeNi	1×10^{-5}	5×10^{15}	31	alloyed
AuGePt	4×10^{-7}	7×10^{17}	32	e-beam pulse annealed
AuGeIn	1.3×10^{-6}	1×10^{17}	33	e-beam pulse annealed
AuGeNi	3×10^{-4}	2.5×10^{15}	34	alloyed
AuGeNi	3.6×10^{-6}	1×10^{16}	35	alloyed
AuTeNi	5×10^{-7}	1×10^{17}	36	alloyed
Au/Ge/GaAs	1×10^{-7}	1.5×10^{18}	37	Ge heterstructure/nonalloyed
$In_xGa_{1-x}As$	5×10^{-7}	2×10^{17}	38	graded gap/nonalloyed
SLS GaAs/InAs	8.5×10^{-8}	5×10^{17}	39	strained layer superlattice

VIII. CONCLUSION

The electron tail lowering limits the usefulness of the standard emission equations described in Secs. I–III. Especially for good ohmic contacts, the thermionic field or field emission theories are not applicable. To assign a certain potential barrier height to measured specific contact resistances with the use of these theories does not represent any physical reality. Especially for the estimation of lower contact resistance limits, classical theories fail to give an accurate limit. The present paper derives an expression for a fundamental lower-contact-resistance limit for metal-semiconductor barriers which is also immediately applicable to semiconductor-semiconductor junctions like n-n^+ barriers and the experimental data for it fits well. It turns out that the semiconductor bulk doping is responsible for the resistance limitation in ohmic contacts. The previously known N_d^{-1} doping dependence of the contact resistance for nondegenerate semiconductors could be verified. For degenerate semiconductors, a deviation from this law is evident and the ohmic contact resistance tends to saturate at increasing doping concentrations, forming a lower-contact-resistance limit for usual physically possible doping concentrations. Si and Ge show the lowest-resistance limits which are according to the present theory at about $3\text{–}4\times10^{-9}\ \Omega\,cm^2$ at a bulk doping concentration of $N_d = 10^{20}\ cm^{-3}$. GaAs and InP show a contact resistance limit of about $1\times10^{-8}\ \Omega\,cm^2$ and InAs and InSb have a $1.5\times10^{-8}\ \Omega\,cm^2$ limit, all at doping concentrations of $1\times10^{20}\ cm^{-3}$. The influence of the n-n^+ barrier on the total contact resistance is shown, together with proof that thermionic emission is the prevailing current transport in n-n^+ junctions and that the doping step is responsible for the limitation effect of the contact resistance. The derived contact resistance limit is of fundamental nature and must be accounted for in future developments.

ACKNOWLEDGMENTS

Special thanks to Lili He, Quanxi Jia, Zhiqing Shi, and Kaili Jiao for their cooperation and thoughtful discussions.

[1] R. Stratton, Phys. Rev. **125**, 67 (1962).
[2] F. A. Padovani and R. Stratton, Solid State Electron **9**, 695 (1966).
[3] R. Stratton, J. Phys. Chem. Solids **23**, 177 (1962).
[4] C. R. Crowell and V. L. Rideout, Solid State Electron. **12**, 89 (1969).
[5] A. Y. C. Yu, Solid State Electron. **13**, 239 (1970).
[6] C. R. Crowell and S. M. Sze, Solid State Electron. **9**, 1035 (1966).
[7] C. Y. Chang and S. M. Sze, Solid State Electron. **13**, 727 (1970).
[8] C. Y. Chang, Y. K. Fang, and S. M. Sze, Solid State Electron. **14**, 541 (1971).
[9] B. Pellegrini, Phys. Rev. B **7**, 5299 (1973).
[10] B. Pellegrini, Solid State Electron. **17**, 217 (1974).
[11] K. Shenai and R. W. Dutton, IEEE Trans. Electron Devices **ED-35**, 468 (1988).
[12] K. Shenai, IEEE Trans. Electron Devices **ED-34**, 1642 (1987).
[13] W. Franz, in *Handbuch der Physik*, edited by S. Flugge (Springer, Berlin, 1956), Vol. 18, p. 155.
[14] M. Braslau, J. Vac. Sci. Technol. **19**, 803 (1981).
[15] R. S. Popović, Solid State Electron. **21**, 1133 (1978).
[16] R. P. Gupta and W. S. Khokle, IEEE Electron Device Lett. **EDL-6**, 300 (1985).
[17] G. Brezeanu, C. Cabuz, D. Dascalu, and P. A. Dan, Solid State Electron. **30**, 527 (1987).
[18] F. Vidimari, Electron. Lett. **15**, 674 (1979).
[19] D. Wu, D. Wang, and K. Heime, Solid State Electron. **29**, 486 (1986).
[20] D. Wu and K. Heime, Electron. Lett. **18**, 940 (1982).
[21] C. R. Crowell, Solid State Electron. **8**, 395 (1965).
[22] C. R. Crowell, Solid State Electron. **12**, 55 (1969).
[23] L. Reggiani, *Hot-Electron Transport in Semiconductors*, Vol. 58 of *Topics in Applied Physics* (Springer, New York, 1985), pp. 55–60.
[24] T. Inada, S. Kato, T. Hara, and N. Toyoda, J. Appl. Phys. **50**, 4466 (1979).
[25] D. C. Marvin, N. A. Ives, and M. S. Leung, J. Appl. Phys. **58**, 2659 (1985).
[26] R. H. Cox and H. Strack, Solid State Electron. **10**, 1213 (1967).
[27] L. C. Wang, X. Z.Wang, S. S. Lau, T. Sands, W. K. Chan, and T. F. Kuech, Appl. Phys. Lett. **56**, 2129 (1990).
[28] A. Christou, Solid State Electron. **22**, 141 (1979).
[29] D. A. Allan and S. C. Thorp, Physica B + C **129**, 445 (1985).

[30] C. L. Chen, L. J. Mahoney, M. C. Finn, R. C. Brooks, A. Chu, and J. G. Mavroides, Appl. Phys. Lett. **48**, 535 (1986).
[31] A. Piotrowska, A. Guivarch, and G. Pelous, Solid State Electron. **26**, 179 (1983).
[32] J. L. Tandon, *Laser and Electron Beam Processing of Materials* (Academic, New York, 1980), p. 487.
[33] G. Eckhardt, *Laser and Electron Beam Processing of Materials* (Academic, New York, 1980), p. 467.
[34] G. Y. Robinson, Solid State Electron. **18**, 331 (1975).
[35] M. Otsubo, H. Kumabe, and H. Miki, Solid State Electron. **20**, 617 (1977).
[36] C. Ghosh, P. Yenigalla, and K. Atkins, IEEE Electron Device Lett. **EDL-4**, 301 (1983).
[37] R. Stall, C. E. C. Wood, K. Board, and L. F. Eastman, Electron. Lett. **15**, 800 (1979).
[38] J. M. Woodall, J. L. Freeouf, G. G. Pettit, and P. Kirchner, J. Vac. Sci. Technol. **19**, 626 (1981).
[39] N. S. Kumar, J. I. Chyi, C. K. Peng, and H. Morkoc, Appl. Phys. Lett. **55**, 775 (1989).
[40] T. Nittono, H. Ito, O. Nakajima, and T. Ishibashi, Jpn. J. Appl. Phys. **27**, 1718 (1988).
[41] C. K. Peng, J. Chen, J. Chyi, and H. Morkoc, J. Appl. Phys. **64**, 429 (1988).